

# Critical Behavior of the Three-Dimensional Ising Spin Glass.

H.G. Ballesteros<sup>1</sup>, A. Cruz<sup>2</sup>, L.A. Fernández<sup>1</sup>, V. Martín-Mayor<sup>3</sup>, J. Pech<sup>2</sup>,  
J.J. Ruiz-Lorenzo<sup>4</sup>, A. Tarancón<sup>2</sup>, P. Téllez<sup>2</sup>, C.L. Ullod<sup>2</sup>, C. Ungil<sup>2</sup>.

<sup>1</sup> *Depto. de Física Teórica, Facultad de CC. Físicas, Universidad Complutense de Madrid, 28040 Madrid, Spain.*

<sup>2</sup> *Depto. de Física Teórica, Facultad de Ciencias, Universidad de Zaragoza, 50009 Zaragoza, Spain.*

<sup>3</sup> *Dip. di Fisica, Università di Roma "La Sapienza" and INFN, Ple. Aldo Moro 2, 00185 Roma, Italy.*

<sup>4</sup> *Depto. de Física, Facultad de Ciencias, Universidad de Extremadura, 06071 Badajoz, Spain.*

(February 1, 2008)

PACS number(s): 75.50.Lk, 64.60.Cn, 05.50.+q

We have simulated, using parallel tempering, the three dimensional Ising spin glass model with binary couplings in a helicoidal geometry. The largest lattice ( $L = 20$ ) has been studied using a dedicated computer (the SUE machine). We have obtained, measuring the correlation length in the critical region, a strong evidence for a second-order finite temperature phase transition ruling out other possible scenarios like a Kosterlitz-Thouless phase transition. Precise values for the  $\nu$  and  $\eta$  critical exponents are also presented.

## I. INTRODUCTION

The study of spin-glasses [1], beyond their own physical relevance, has opened new ways to Statistical Physics. The solution [2] of the Sherrington-Kirkpatrick model, that describes spin-glasses living in infinite dimensions, allowed the introduction of a new set of ideas that have found applications in very different contexts, like Optimization, Neural Networks, and so on. Yet the applicability of the rich infinite-dimensional physical picture to describe the low-temperature physics of three-dimensional spin-glass materials (like, for instance, Cu Mn, Ag Mn,  $\text{Eu}_x\text{Sr}_{1-x}\text{S}$ , see [3]) is still controversial [4]. Furthermore, a rather simpler question, *what is the nature of the spin-glass phase transition?*, has not yet found a fully satisfactory answer. Although the very existence of a phase transition has been questioned, from the experimental side, there is now a wide consensus on its existence, as signalled by the behavior of the non-linear susceptibility [5].

On the other hand, the theoretical approach is almost limited to the Monte Carlo simulation of the Edwards-Anderson model, given the enormous difficulties found when using field-theoretic renormalization group techniques [6]. Recent numerical simulations [7–11] have found indications of a finite-temperature phase transition, which has been confirmed in Ref. [12]. However, the possibility [10] of a Kosterlitz-Thouless like phase transition (an exponential divergence of the correlation-length at the critical temperature followed by a line of critical points) could *not* be excluded [12]. Even so, critical-exponent estimates that could be compared with experiments were obtained [7–15] by assuming power-law divergences at the critical temperature (i.e., *non* Kosterlitz-Thouless behavior). However, the statistical errors of those estimates (10% for the correlation-length exponent  $\nu$ , and 15 % in the anomalous dimension,  $\eta$ ), and that of the critical temperature estimate seems poor compared to similar computations for ordered systems, which is due to the numerical difficulties encountered on the simulation of the Edwards-Anderson model. In fact, the issue (crucial for accurate calculations of critical exponents) of the scaling corrections has not been addressed in previous works, exception made of Ref. [12].

In this work, we shall perform a detailed study of the critical behavior of the Edwards-Anderson model. The numerical simulations have been in part performed on a dedicated computer (the SUE machine, see below for more details), on which we have been able to thermalize 6920 samples of  $20^3$  lattices at the critical temperature, the largest thermalized lattices in previous studies at similar temperatures being  $16^3$ . For the thermalization deep inside the critical region we have used the Monte Carlo exchange method (also known as parallel tempering) [16–18].

Our study shares with Ref. [12] the definition of the finite-lattice correlation-length [19], and a heavy use of the Finite-Size Scaling (FSS) Ansatz [20]. Yet, both analyses are rather different. Ref. [12] uses the techniques of Ref. [21] to extrapolate the measures taken on lattices which are small compared with the correlation-length, to the thermodynamic limit. On the other hand, we use the quotient method [22], where measures taken on two lattices are compared at the temperature at which the correlation-length measured in units of the lattice-size coincides for both.

For the particular problem of spin-glasses, the method of Ref. [12] has the advantage of not requiring the thermalization of large lattices at large correlation-lengths (the dynamical critical exponent for the three dimensional Ising spin glass in the critical region is near 7 [23]). On the other hand, the quotient method offers the possibility of extremely precise determinations of critical exponents and temperatures, and a rather transparent control of scaling-corrections, also in disordered systems [24]. The main drawback for its use on spin-glass systems is that it requires measures taken on several pairs of lattice of widely different sizes at the critical temperature, which is rather difficult due to the above mentioned thermalization problems [25].

We obtain very precise estimates for critical exponents which are compared with the estimates of other groups and with available experimental results. The issue of scaling-corrections will be discussed, and a rough estimate of  $\omega$  (the correction-to-the-scaling exponent) will be obtained.

An additional bonus of our computational strategy is that high-quality data for the spin-glass correlation length are generated on large lattices at the critical region. This allows for a detailed comparison with the archetypical model displaying a Kosterlitz-Thouless phase transition, the XY model in two dimensions (for which a cluster method is available, making the simulation almost costless). The finite-size scaling behavior of both models is not only quantitatively but qualitatively different. We therefore present strong evidence against Kosterlitz-Thouless behavior on the Edwards-Anderson model.

Finally, we also consider the question of the appropriate cumulant for the study of the spin-glass phase transition. In Ref. [26] it has been argued that the Binder cumulant [27] works poorly, in marked contrast with ordered systems. It is also claimed that the cumulant  $G$  introduced in Ref. [28] for the study of systems without time-reversal symmetry, see Eq.(7), does a better job. We shall show that it suffers from similar scaling corrections but of opposite *sign*, so that its crossings happens at temperatures higher than the critical point. This is rather advantageous from the point of view of thermalization. On the other hand, its measures are far noisier than the ones of the finite-lattice correlation-length, and it also suffers from stronger corrections to scaling.

The large statistics needed to obtain precise results on larger lattices has been possible by the use of a dedicated computer based on programmable components. Details about the machine can be seen in Refs. [29–31]. SUE, for Spin Update Engine, consists of twelve boards attached to a PC. Each of these boards contains programmable devices and memories, allowing the simulation of eight lattices of size up to  $L = 60$ . The presence in each board of a component dedicated to random number generation allows the use of the Heat Bath algorithm. During the simulation, Schwinger-Dyson equations [32,33] were used to check for the correctness of the random-number sequences. Periodically, the spin configurations are downloaded to the PC, where the measures are performed and stored. When using the parallel tempering scheme, the PC controls the mechanism, interchanging the configurations corresponding to adjacent temperatures when appropriate. The update speed of the whole system is 0.22 ns/spin, one hundred times faster than one Alpha EV5, 600 MHz processor running multi-spin code.

The layout of the rest of this paper is as follows. In the next section we introduce the model, the definition of the observables and we review the basis of our Finite Size Scaling (FSS) method. The third section is devoted to analyze the statistical quality of our data, in particular we discuss the thermalization, the parallel tempering parameters and our choice of the number of samples versus number of steps inside one sample. The discussion of our numerical results follows, where we compare them with previous numerical simulations and experiments. We end the paper with the conclusions.

## II. MODEL, OBSERVABLES AND THE FSS METHOD

We have studied the three dimensional Ising spin glass defined on a cubic lattice ( $L \times L \times L$ ) with helicoidal boundary conditions [34], whose Hamiltonian is

$$\mathcal{H} = - \sum_{\langle i,j \rangle} \sigma_i J_{ij} \sigma_j . \quad (1)$$

The volume of the system is  $V = L^3$ ,  $\sigma_i$  are Ising variables,  $J_{ij}$  (uncorrelated quenched disorder) are  $\pm 1$  with equal probability, and the sum is extended to all pairs of nearest neighbors. Due to the quenched nature of the disorder, one needs to perform first the thermal average for a given configuration of the  $J_{ij}$  (denoted by  $\langle \dots \rangle$  hereafter), and later the average over the disorder realization (that will be indicated by

an overline). The choice of helicoidal boundary conditions is mandatory (for us) because the hardware of the SUE machine has been optimized for them.

We have simulated the smaller lattice sizes ( $L = 5$  and  $10$ ) in parallel machines built of Pentium-Pro processors (the RTNN machines) using multi-spin coding. We have checked that the  $L = 10$  and  $L = 5$  lattices are properly thermalized with a standard Heat Bath method (without parallel tempering). The larger lattice ( $L = 20$ ) has been simulated in the SUE machine using parallel tempering and Heat Bath.

We shall describe in depth the thermalization test and the total statistics achieved in the next section.

### A. Observables

It is well known that observables in spin-glasses need to be defined in terms of real replicas, that is, for every disorder realization, one considers two thermally independent copies of the system  $\{s_i^{(1)}, s_i^{(2)}\}$ . Observables are most easily defined in terms of a spin-like field, the so-called overlap field:

$$q_i = s_i^{(1)} s_i^{(2)}. \quad (2)$$

The total overlap is the lattice average of the  $q_i$

$$q = \frac{1}{V} \sum_i q_i, \quad (3)$$

while the (non-connected) spin-glass susceptibility is

$$\chi_q = V \overline{\langle q^2 \rangle}. \quad (4)$$

In Finite-Size Scaling studies, it is useful to have dimensionless quantities, that go to a constant value at the critical temperature. A standard example of such a quantity is the Binder cumulant

$$g_4 = \frac{3}{2} - \frac{1}{2} \frac{\overline{\langle q^4 \rangle}}{\overline{\langle q^2 \rangle}^2}. \quad (5)$$

Other example is the  $g_2$  cumulant [24], that measures the lack of self-averageness of the spin-glass susceptibility

$$g_2 = \frac{\overline{\langle q^2 \rangle^2} - \overline{\langle q^2 \rangle}^2}{\overline{\langle q^2 \rangle}^2}. \quad (6)$$

Of course, any smooth function of these two dimensionless quantities,  $g_2$  and  $g_4$ , is dimensionless itself. In Ref. [28] it was proposed to study the cumulant  $G$

$$G = \frac{g_2}{2 - 2g_4} \quad (7)$$

because it exhibits a significant reduction of scaling corrections. It has also been argued in Ref. [26] that  $G$  can be extremely helpful for the characterization of the spin-glass phase, but this issue is out of the scope of this work. However all the above defined dimensionless quantities,  $g_4$ ,  $g_2$  and  $G$ , require the evaluation of a four-point correlation function, which is statistically a much noisier quantity than a two-point one. One observable of this kind is the correlation-length, which is defined in terms of the two-point correlation function, and its quotient with the lattice size is again dimensionless. We therefore are faced with the problem of defining a correlation-length on a finite lattice. In Ref. [19] it was shown how to do it, from the following considerations. Let us call  $C(\mathbf{r})$  the correlation function of the overlap field,

$$C(\mathbf{r}) = \frac{1}{V} \sum_i \overline{\langle q_i q_{i+\mathbf{r}} \rangle} \quad (8)$$

and  $\hat{C}(\mathbf{k})$  its Fourier transform. Notice that the spin glass susceptibility is simply  $\hat{C}(0)$ . Then, inside the critical region on the paramagnetic side and in the thermodynamical limit, one has

$$\hat{C}(\mathbf{k}) \propto \frac{1}{k^2 + \xi^{-2}}, \quad \|\mathbf{k}\| \ll \xi^{-1}, \quad (9)$$

$$\xi^{-2} = -\frac{1}{\hat{C}} \left. \frac{\partial \hat{C}}{\partial k^2} \right|_{k^2=0}. \quad (10)$$

On a finite lattice, the momentum is discretized, and one uses [19] a finite-differences approximation to Eq.(10),

$$\xi^2 = \frac{1}{4 [\sin^2(k_m^x/2) + \sin^2(k_m^y/2) + \sin^2(k_m^z/2)]} \left[ \frac{\chi_q}{\hat{C}(\mathbf{k}_m)} - 1 \right], \quad (11)$$

where  $\chi_q$  was defined in Eq. (4) and  $\mathbf{k}_m$  is the minimum wave-vector allowed for the used boundary conditions, which in our case is  $\mathbf{k}_m = (2\pi/L, 2\pi/L^2, 2\pi/L^3)$ . Of course, Eq.(10) holds on the thermodynamic limit ( $L \gg \xi$ ) of the paramagnetic phase. As we do not use connected correlation functions,  $\xi$  has sense as a correlation length only for  $T > T_c$ .

We can study the scaling behavior of the finite-lattice definition (11) on a critical point, where the correlation function decays (in  $D$  dimensions) as  $r^{-(D-2+\eta)}$ . The behavior of the Fourier transform of the correlation function for large  $L$  in three dimensions is given by

$$\hat{C}(k) \sim \int_0^L dr r^{1-\eta} \frac{\sin(kr)}{kr}, \quad (12)$$

and one finds that  $\chi_q/\hat{C}(\mathbf{k}_m)$  goes to a constant value, larger than unity, because  $\|\mathbf{k}_m\| = \mathcal{O}(1/L)$ . Furthermore,  $\xi/L$  tends to a universal constant at a critical point (like the Binder cumulant  $g_4$ ). Moreover, on a broken-symmetry phase, where the fluctuations of the order parameter are not critical, one has  $\chi_q = \mathcal{O}(V)$ , while  $\hat{C}(\mathbf{k}_m) = \mathcal{O}(1)$ . Therefore the full description of the scaling behavior of  $\xi/L$  is as follows. Let  $\xi_\infty$  be the correlation-length on the infinite lattice: in the paramagnetic phase, for  $L \gg \xi_\infty$ , one has  $\xi/L = \mathcal{O}(1/L)$ . On the FSS region, where  $\xi_\infty \geq L$ ,  $\xi/L = \mathcal{O}(1)$ , while on a broken-symmetry phase on a lattice larger than the scale of the fluctuations,  $\xi/L = \mathcal{O}(L^{D/2})$ . Consequently, if one plots  $\xi/L$  for several lattice sizes as a function of temperature, the different graphics will cross at the critical temperature.

Finally, a very useful quantity is the value of the Hamiltonian, which is used to measure the derivatives of a generic observable,  $O$ , with respect to the inverse temperature  $\beta$

$$\partial_\beta \langle O \rangle = \langle O \mathcal{H}^{(1)} + O \mathcal{H}^{(2)} \rangle - \langle O \rangle \langle \mathcal{H}^{(1)} + \mathcal{H}^{(2)} \rangle, \quad (13)$$

where the <sup>(1)</sup> and <sup>(2)</sup> superscripts refers to the two replicas needed to construct the operator  $O$ . Similarly one generalizes the standard reweighting method [35], that allows to extrapolate the measures taken at  $\beta$  to neighboring values:

$$\langle O \rangle_{\beta+\Delta\beta} = \frac{\langle O e^{\Delta\beta \mathcal{H}^{(1)} + \Delta\beta \mathcal{H}^{(2)}} \rangle_\beta}{\langle e^{\Delta\beta \mathcal{H}^{(1)} + \Delta\beta \mathcal{H}^{(2)}} \rangle_\beta}. \quad (14)$$

## B. The FSS method

We have used the quotient method [22], in order to compute the critical exponents. We recall briefly the basis of this method. Let  $O$  be a quantity diverging in the thermodynamical limit as  $t^{-x_O}$  ( $t = T/T_c - 1$  being the reduced temperature). We can write the dependence of  $O$  on  $L$  and  $t$  in the following way [20]

$$O(L, t) = L^{x_O/\nu} \left[ F_O \left( \frac{L}{\xi(\infty, t)} \right) + \mathcal{O}(L^{-\omega}, \xi^{-\omega}) \right], \quad (15)$$

where  $F_O$  is a (smooth) scaling function and  $(-\omega)$  is the corrections-to-scaling exponent (e.g.,  $\omega$  is the largest negative eigenvalue of the Renormalization Group transformation). This expression contains the

not directly measurable term  $\xi(\infty, t)$ , but if we have a good definition of the correlation length in a finite box  $\xi(L, t)$ , Eq. (15) can be transformed into

$$O(L, t) = L^{x_O/\nu} \left[ G_O \left( \frac{\xi(L, t)}{L} \right) + \mathcal{O}(L^{-\omega}) \right], \quad (16)$$

where  $G_O$  is a smooth function related with  $F_O$  and  $F_\xi$  and the term  $\xi_\infty^{-\omega}$  has been neglected because we are simulating deep in the scaling region. We consider the quotient of measures taken in lattices  $L$  and  $sL$  at the same temperature

$$Q_O(s, L, t) = \frac{O(sL, t)}{O(L, t)}. \quad (17)$$

Then, the main formula of the quotient method is

$$Q_O|_{Q_\xi=s} = s^{x_O/\nu} + \mathcal{O}(L^{-\omega}), \quad (18)$$

i.e., we compute the reduced temperature  $t$ , at which the correlation length verifies  $\xi(sL, t)/\xi(L, t) = s$  and then the quotient between  $O(sL, t)$  and  $O(L, t)$ . In particular, we apply formula (18) to the overlap susceptibility,  $\chi_q$ , and the  $\beta$ -derivative of the correlation length,  $\partial_\beta \xi$ , whose associated exponents are:

$$x_{\partial_\beta \xi} = 1 + \nu, \quad (19)$$

$$x_{\chi_q} = (2 - \eta)\nu. \quad (20)$$

Notice that  $Q_O|_{Q_\xi=s}$  can be measured with great precision because of the large statistical correlation between  $Q_O$  and  $Q_\xi$ . It is very important that in order to use Eq.(18) one does not need the infinite-volume extrapolation for the critical temperature but, instead, a reweighting method [35] is crucial to fine-tune the  $Q_\xi = s$  condition. From Eq.(18) one directly extracts *effective* exponents (i.e., lattice-size dependent) and later on checks for scaling-corrections. Another advantage of the quotient method is that the crossing temperature for  $\xi/L$  (i.e., the temperature for which  $Q_\xi = s$ ) scales as

$$t_{s,L}^{\text{crossing}} \propto L^{-\omega-1/\nu}, \quad (21)$$

so that one works a factor  $L^{-\omega}$  closer to the critical point than with other FSS methods, such as measuring at the maximum of (say) the connected susceptibility. This puts considerably less stress on the quality of the reweighting method. It should also be mentioned that one could modify Eq.(18), and measure at the crossing point of a cumulant such as  $g_4$ ,  $g_2$  or  $G$ . The results should coincide, up to scaling corrections, but given the better statistical quality of the measures of  $\xi/L$ , the error bars would significantly grow.

### III. STATISTICAL QUALITY OF THE DATA

When designing a simulation for a disordered model, one needs to carefully consider how many measures will be taken on each sample,  $N_I$ , and the number of samples to be simulated  $N_S$ . Two competing effects need to be balanced for this. On the first place, from the error analysis of a generic observable,  $O$ , one has ( $\eta$  is a Gaussian number of zero-mean and unit variance)

$$\left( \overline{\langle O \rangle}^{\text{MonteCarlo}} - \overline{\langle O \rangle} \right)^2 = \frac{\eta}{N_S} \left( \sigma_{S,O}^2 + \frac{2\tau_O \sigma_{I,O}^2}{N_I} \right), \quad (22)$$

where  $\sigma_{S,O}$  is the variance between different samples of the exact thermal averages,  $\sigma_{I,O}$  is the disorder-averaged variance for the measures on a sample, and  $\tau_O$  is an averaged (integrated) autocorrelation time [36]. This shows that the optimum value of  $N_I$  cannot be much greater than  $2\tau_O \sigma_{I,O}^2 / \sigma_S^2$ . On the other hand, when evaluating non-linear functions of thermal-averages, as in Eqs.(13,14), a bias of order  $2\tau_O/N_I$  is present (for the reweighted measures a bias polynomial in  $2\tau_O/N_I$  is expected). If  $\sqrt{N_S}$  is not much smaller than  $N_I$ , the statistical errors will shrink enough as to uncover the bias, and we have two conflicting goals for the optimization of  $N_I$  and  $N_S$ . In order to solve the dilemma, we have followed

$L$	$N_S$	$N_{HB}$	$N_I$
5	40 000	200 000	200
10	40 000	500 000	500
20	6 920	6 553 600	400

TABLE I. Statistics used. For each sample, we run  $N_{HB}$  Heat Bath sweeps and perform  $N_I$  measures. Each sample is previously thermalized with  $N_{HB}$  iterations. In the  $L = 20$  lattice, we carry out a parallel tempering step after each measure.

the same procedure as in Ref. [24] to eliminate the bias. One first evaluate the non-linear function with the full set of data, then divides the data in two sets of length  $N_I/2$  for each of which the function is evaluated and the two results are averaged, and the procedure is repeated dividing the data in four sets of  $N_I/4$  measures. We thus have three estimates of the non-linear function, with bias of order  $1/N_I$ ,  $2/N_I$  and  $4/N_I$  respectively. The three estimates are used in a quadratic (in  $1/N_I$ ) extrapolation to  $1/N_I = 0$ , which is later on averaged over the disorder. In order to have meaningful results from this extrapolation, it is crucial that  $2\tau/N_I$  be a reasonably small number. The values of  $N_I$  and  $N_S$  for our simulations are shown in table I. We remark that we need also to balance the Heat-bath steps, done by the dedicated machine SUE, and the parallel tempering steps done by the PC which handles SUE (during this time SUE is stopped).

With our simulation strategy ( $N_I \ll N_S$ ), it is crucial to check that the system is sufficiently thermalized while taking measures. A very efficient algorithm for thermalizing spin-glass systems is parallel tempering [16–18]. In order to obtain an efficient parallel tempering we must select a range of  $\beta$  values, and the number of intervals in this range. The range is fixed in the following way: The faster decorrelation time is at the lowest  $\beta$ ; as we run a fixed number of iteration between parallel tempering sweeps, this number must be greater than the autocorrelation time at this  $\beta$  value. For these values of  $\beta$ , away from the transition point, the correlation length  $\xi$  is (almost)  $L$ -independent. Running around  $10^4$  sweeps and considering that the correlation time grows as  $\xi^7$  [23] we use finally  $\beta_{\min} = 0.70$ . The largest value must be a bit over the crossing point, which we had estimated previously around 0.88. We use then  $\beta_{\max} = 0.92$ . The number of  $\beta$  values is fixed by controlling that the probability of changes in the parallel tempering is significant. This number depends on  $L$  and for  $L = 20$  we have used 12 values of  $\beta$ , obtaining a probability of transition around 30%. All the systems are a significant time in the lower  $\beta$  values, where decorrelation is faster.

A first thermalization check is summarized in Fig. 1. The measures taken on a sample are divided in twenty blocks, and the correlation-length and the spin-glass susceptibility are calculated with these blocks. No thermalization bias can be resolved after the fifth block at the lowest temperature. However, the first ten blocks have been discarded for safety.

Yet the results in Fig. 1 do not really show that we are collecting a reasonable number of measures on each sample (so that  $2\tau/N_I$  is small), because the time needed to obtain a thermalized measure is not straightforwardly linked to the time needed to obtain an independent measure. In fact, the latter is related with the time needed to overcome free-energy barriers, in order to visit different relevant regions of phase-space [11], while the former is related with the time needed to reach *at least one* relevant region of phase space, because the huge number of samples avoids a biased estimation. A better test comes from the smoothness of the bias-corrected reweighting extrapolation. In Fig. 2 we show the extrapolated values  $\xi/L$ ,  $g_4$  and  $\chi_q$  from each of the  $\beta_i$  of the parallel tempering (alternatively in dotted and dashed lines). The mismatch between different extrapolations is much smaller than the error bars, which is due to the fact that the same samples are being simulated for all  $\beta_i$  values. In fact, for  $N_I \rightarrow \infty$  the mismatch would completely disappear, while the statistical error bars would not be smaller unless  $N_S$  grows (see Eq. (22)).

Finally, along the simulation the Schwinger-Dyson equations have been checked finding a perfect agreement. For instance, the equation in [33] holds within a 0.04% for the  $L = 20$  lattice.

#### IV. NUMERICAL RESULTS

Once a set of measures of the finite-lattice correlation-length is at our disposal, the first question one can answer regards the nature of the spin-glass phase transition in three dimensions. Indeed, if the

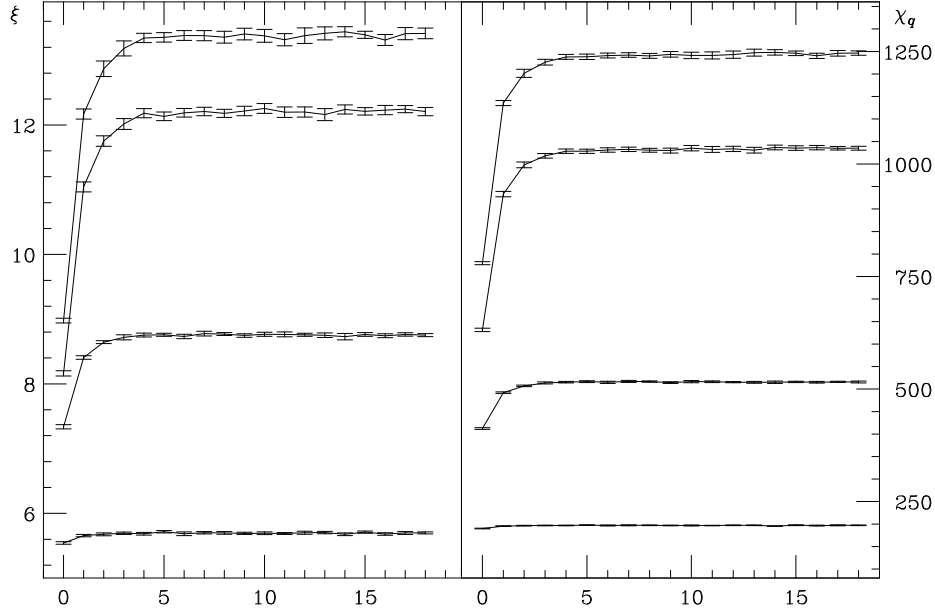


FIG. 1. Mean values of the susceptibility and correlation length in the  $L = 20$  lattice for successive bins of 40 measures, for several  $\beta_i$  values in  $L = 20$  (from top to bottom they correspond to  $\beta_{11}$ ,  $\beta_9$ ,  $\beta_4$  and  $\beta_0$ , respectively). We remark that  $\beta_{11} = \beta_{\max} = 0.92$  corresponds with our coldest temperature. In the following, we discard the first 10 bins and average the remaining 10.

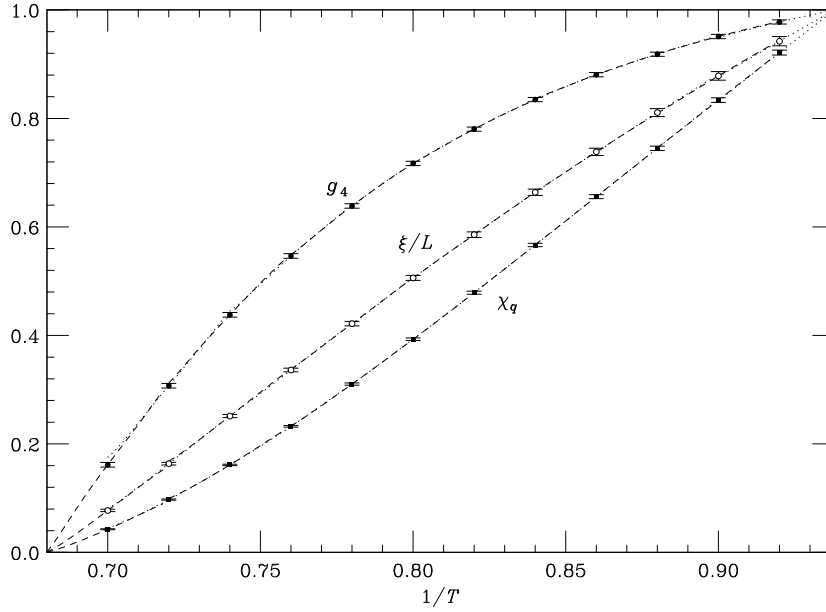


FIG. 2. Correlation length, susceptibility and  $g_4$  cumulant for the  $L = 20$  lattice, as obtained from the extrapolation method of Eq.(14), corrected for bias. We show the results for all the twelve  $\beta$  values of the simulation (point with error bars) together with the extrapolation (alternatively shown in dashed and dotted lines). The curves have been linearly scaled to fit in the figure.

Kosterlitz-Thouless scenario was realized,  $\xi/L$  on the  $L \rightarrow \infty$  limit, would be zero for temperatures higher than the critical one, and then it would abruptly jump at the critical temperature to a finite value. For lower temperatures, since the system would still be critical, it would keep a finite value, presumably

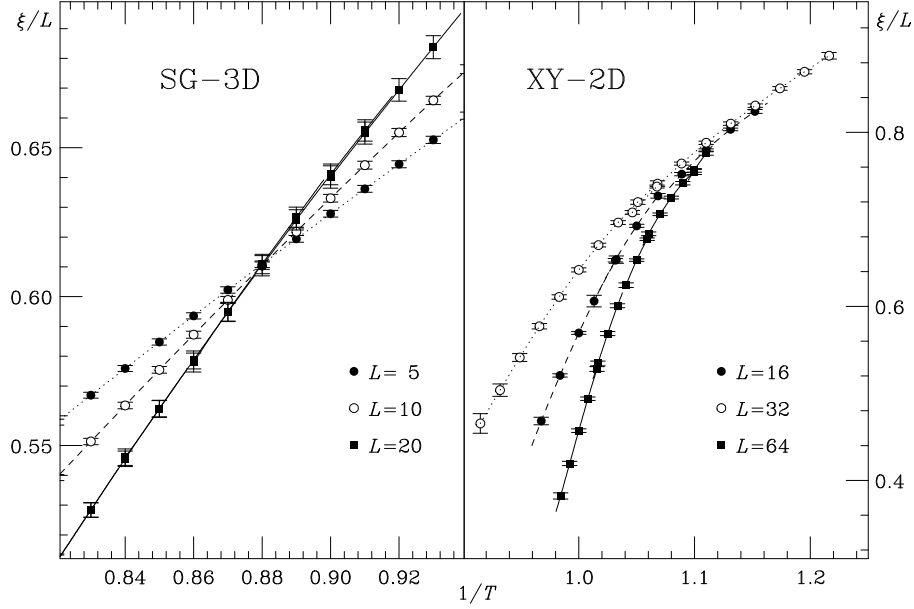


FIG. 3. Correlation length in units of the lattice size for the 3D Edwards-Anderson model (left), and for the 2D XY-model that displays a Kosterlitz-Thouless phase transition.

growing with lowering temperatures. On a finite lattice,  $\xi/L$  would be a decreasing function of  $L$  on the paramagnetic phase, and in the critical region (from the critical temperature to lower ones), it would have a  $L$  independent value, according to the FSS Ansatz, up to scaling corrections. Therefore, in the most economic scenario, where scaling corrections are small, the different  $\xi/L$  curves do not cross, but simply merge in the low-temperature region.

In Fig. 3, we plot  $\xi/L$  for the Edwards-Anderson model in three dimension and for the XY model in two dimensions (whose simulation is almost costless in computer time [37]). We see that while the XY model follows quite closely the above sketched behavior, the Edwards-Anderson model has a very neat crossing. Therefore, one may conclude that the Kosterlitz-Thouless scenario is ruled out by the data, unless scaling-corrections of a very exotic nature would be present. Notice, that for the two dimensional XY model,  $\xi/L$  and the Binder cumulant behave in the same way with  $L$  and  $T$  [10].

This is an interesting point to compare the behavior of the  $g_4$  and  $G$  cumulants, defined above, with  $\xi/L$ . From Fig. 4, it is clear that the measures for  $G$  are much noisier than for  $\xi/L$ . Moreover, also the scaling corrections are larger, as made evident by the large shift between the crossing of the 5 and 20 lattice, and the crossing of the 10 and 20 lattice. The scaling corrections for  $G$  and  $g_4$  are of opposite signs, so that one can safely conclude that the real critical point is bracketed by this two sets of crossing-points.

For the critical exponents, our results found using Eq. (18) are displayed in table II. Finite-size scaling corrections cannot be resolved within errors, specially if one realizes that the results for the (5, 10) pair are anticorrelated with the results for the (10, 20) pair (the measure in  $L = 10$  appear once in the numerator and the other time in the denominator of Eq.(18)). We take as our final estimate our results for the (10, 20) pair, that can be compared with the most recent experimental measures and with other numerical calculations displayed in table III. It would be very interesting to check that systematic errors due to finite-size effects are smaller than the statistical ones. This would require to parametrize the scaling corrections, and therefore to have precise measures on a wide range of lattice sizes. Unfortunately, the huge

$L$	$T_c$	$\nu$	$\eta$
(5,10)	1.134(9)	2.39(7)	-0.353(9)
(10,20)	1.138(10)	2.15(15)	-0.337(15)

TABLE II. Critical exponents computed from the crossing points of  $\xi/L$  for  $(L, 2L)$  pairs.

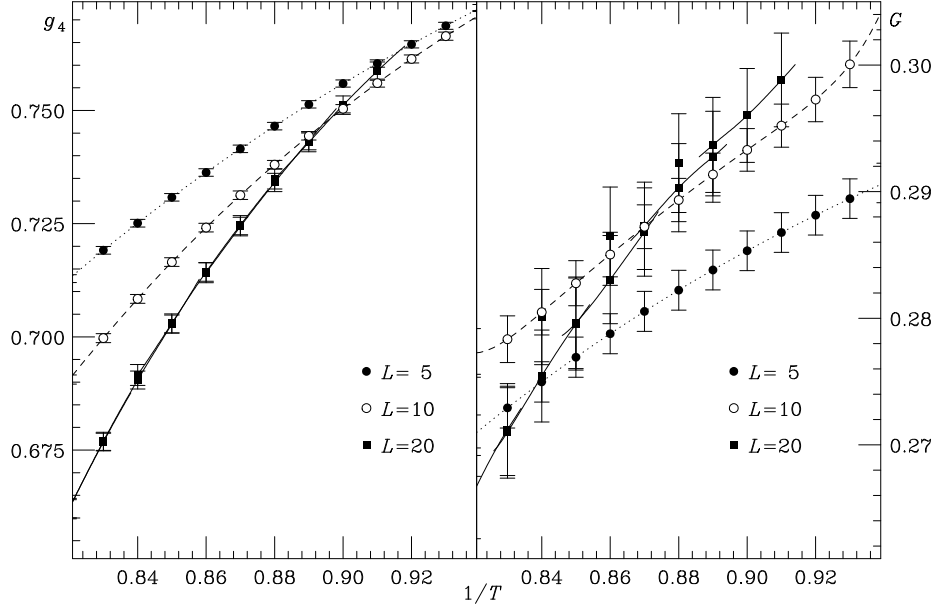


FIG. 4. Cumulants  $g_4$  and  $G$  for lattices  $L = 5, 10, 20$  versus inverse temperature.

dynamical critical exponent of the available simulation algorithms for this model makes extremely difficult to thermalize, at the critical point, lattices larger than  $L = 20$  with present technological capabilities.

Nevertheless, it is possible to obtain information about  $\omega$  studying the quotients of cumulants  $Q_g$  at the point where  $\xi/L$  crosses. At this point,  $Q_g$  should be 1 up to scaling corrections and can be parameterized as

$$Q_g = 1 + A_g L^{-\omega}. \quad (23)$$

Before presenting our results for  $\omega$ , let us recall the values obtained by Palassini and Caracciolo [12] working in the thermodynamical limit. They computed two different scaling-corrections exponents,  $\Delta$  and  $\theta$ . These exponents are obtained from the asymptotic formulae that hold in the scaling region in the thermodynamic limit, in the paramagnetic side

$$\chi = A \xi^{2-\eta}(1 + \mathcal{O}(\xi^{-\Delta})), \quad \xi = B |t|^{-\nu}(1 + \mathcal{O}(|t|^\theta)). \quad (24)$$

One can check from the above expressions, that  $\Delta = \omega$  and  $\theta = \omega\nu$ . From their values of  $\Delta$ ,  $\theta$  and  $\nu$  one readily obtains

$$\omega(\Delta) = 1.3^{+0.2}_{-0.3}, \quad \omega(\theta, \nu) = 0.78^{+0.47}_{-0.28}. \quad (25)$$

We have fitted our measures for  $g_4$  and  $g_2$  following (23). We have 4 points for adjusting 3 parameters, but we obtain the value

$$\omega = 0.84^{+0.43}_{-0.37}, \quad (26)$$

with  $\chi^2 = 0.6$ . See Fig. 5 for more details. Although the statistical error is rather large, the compatibility of our result with those displayed in Eq.(25) is reassuring given the difference on the methods. It should be also mentioned that the so called analytic scaling corrections have been neglected, which is, a posteriori, seen to be a reasonable procedure [39].

Finally, we compare our estimate for the critical temperature ( $T_c = 1.138(10)$ ) with that of Ref. [12] ( $T_c = 1.156(15)$ ), the agreement being very good.

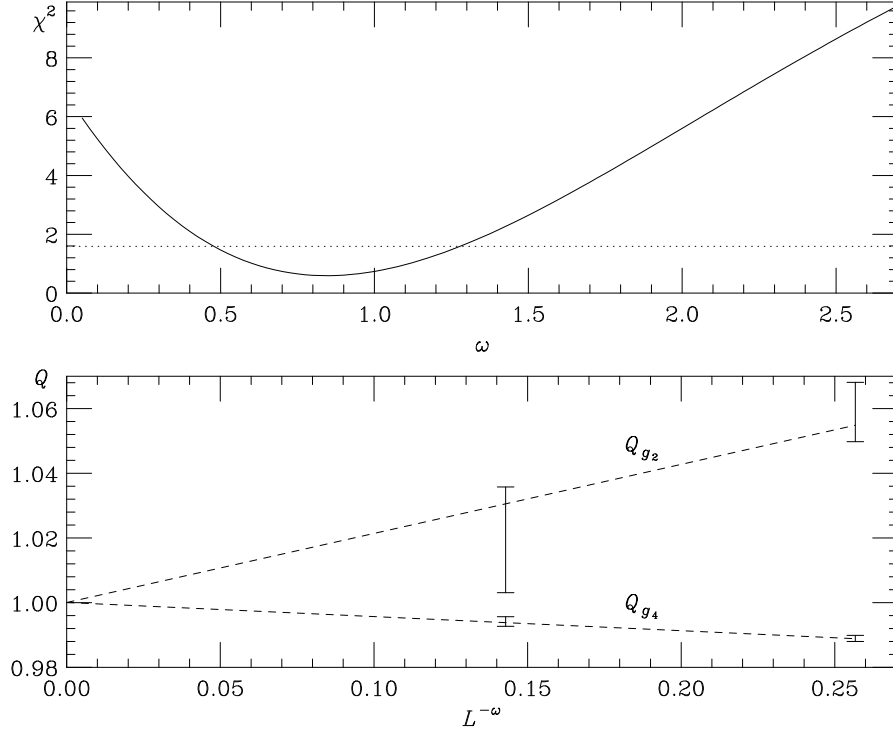


FIG. 5. Quotients of the cumulants  $g_2$  and  $g_4$  for pairs  $(L, 2L)$  as functions of  $L^{-\omega}$  (lower figure). The corrections-to-scaling exponent has been obtained minimizing the  $\chi^2$  function (see (23)) using the full covariance matrix. The horizontal dotted line (in the upper figure) is given by the value of  $\chi^2$  at the minimum plus one.

## V. DISCUSSION AND CONCLUSIONS

We have obtained precise measures of the  $\eta$  and  $\nu$  exponents. Moreover, we have done a study of the corrections to scaling, in particular we have computed the value of the corrections-to-scaling exponent  $\omega$  in a good agreement with the value reported in Ref. [12]. We remark that our statistical error for the  $\eta$  exponent is 5 times smaller than the experimental error for this exponent and 3 times less than the smallest statistical error found in the literature. The fact that our estimates for the (5,10) lattices and the (10,20) pair coincide within statistical errors gives us some confidence on the smallness of the finite size effects, although larger lattices will be needed to make sure that the systematic errors are as small as the statistical ones.

Our comparison with the most recent experimental data [5] is good. The difference between the  $\nu$  exponent measured in experiment and our reported value is 0.046(21), roughly two standard deviations. We note that the  $\nu$  exponent from numerical simulations is systematically above experimental data. The difference for the  $\eta$  exponent is 0.023(71).

The clear crossing of the  $\xi/L$  curves, for different lattice sizes, supports heavily a finite temperature second order phase transition and excludes a Kosterlitz-Thouless like scenario (a phase transition of infinite order or equivalently a line of critical points below the critical temperature).

Our results for the critical exponents for binary  $J$ 's agree well with that obtained simulating Gaussian couplings [9]. However the statistical error are still very large and we lack control on the scaling corrections (completely in the Gaussian “side”). It might be useful to study of the Gaussian EA model with the methodology of this paper but unfortunately the SUE machine is not designed to simulate Gaussian coupling.

## VI. ACKNOWLEDGMENTS

We acknowledge discussions with E. Marinari and G. Parisi. We thank partial financial support from CICyT (AEN97-1680, AEN97-1693, AEN99-0990 and PB98-0842) and DGA (P46/97). V.M-M is a M.E.C. fellow. The computations have been carried out using the RTNN machines (Universidad de Zaragoza and Universidad Complutense de Madrid) and the dedicated machine SUE (Universidad de Zaragoza).

- 
- [1] K. Binder and A. P. Young, Rev. Mod. Phys. **58**, 801 (1986); M. Mézard, G. Parisi and M. A. Virasoro, *Spin Glass Theory and Beyond* (World Scientific, Singapore 1987); K. H. Fisher and J. A. Hertz, *Spin Glasses* (Cambridge University Press, Cambridge U.K. 1991)
  - [2] G. Parisi, Phys. Lett. A **73**, 203 (1979); J. Phys. A **13**, L115 (1980); J. Phys. A **13**, 1101 (1980); J. Phys. A **13** 1887 (1980).
  - [3] J. A. Mydosh, *Spin Glasses: an Experimental Introduction* (Taylor and Francis, London 1993).
  - [4] See, for example, the following recent papers: M. Palassini and A. P. Young, Phys. Rev. Lett. **83**, 5126 (1999); M. Palassini and A. P. Young, cond-mat/0004485; E. Marinari, G. Parisi, F. Ricci-Tersenghi, J. J. Ruiz-Lorenzo and F. Zuliani, J. Stat. Phys. **98**, 973 (2000); E. Marinari and G. Parisi, cond-mat/0005047.
  - [5] K. Gunnarsson et al., Phys. Rev. B **43**, 8199 (1991). See also P. Norblad and P. Svendlidh *Experiments on Spin Glasses* in *Spin Glasses and Random Fields*, edited by A. P. Young. World Scientific (Singapore, 1997).
  - [6] C. de Dominicis, I. Kondor and T. Temesvári, *Beyond the Sherrington-Kirkpatrick Model in Spin Glasses and Random Fields*, edited by A. P. Young. World Scientific (Singapore, 1997).
  - [7] N. Kawashima and A. P. Young, Phys. Rev B **53**, R484 (1996).
  - [8] D. Iñiguez, G. Parisi and J. J. Ruiz-Lorenzo, J. Phys. A **29**, 4337 (1996).
  - [9] E. Marinari, G. Parisi and J. J. Ruiz-Lorenzo, Phys. Rev. B **58**, 14863 (1998).
  - [10] D. Iñiguez, E. Marinari, G. Parisi and J. J. Ruiz-Lorenzo, J. Phys. A **30**, 7337 (1997).
  - [11] B. A. Berg and W. Janke, Phys. Rev. Lett. **80**, 4771 (1998); W. Janke, B. A. Berg and A. Billoire, Ann. Phys.(Leipzig) **7**, 544 (1998).
  - [12] M. Palassini and Caracciolo, Phys. Rev. Lett. **82**, 5128 (1999).
  - [13] A. T. Ogielski, Phys. Rev. B **32**, 7384 (1985).
  - [14] R. N. Bhatt and A. P. Young, Phys. Rev. Lett. **54**, 924 (1985).
  - [15] R. N. Bhatt and A. P. Young, Phys. Rev. B **37**, 5606 (1988).
  - [16] M. Tesi, E. Janse van Resburg, E. Orlandini and S. G. Whittington, J. Stat. Phys. **82**, 155 (1996); K. Hukushima and K. Nemoto, J. Phys. Soc. Jpn. **65**, 1604 (1996).
  - [17] E. Marinari, *Optimized Monte Carlo Methods* in Lecture Notes in Physics 501 (Springer-Verlag, Heidelberg, 1998).
  - [18] E. Marinari, G. Parisi and J. J. Ruiz-Lorenzo, *Numerical Simulations of Spin Glass Systems* in *Spin Glasses and Random Fields*, edited by A. P. Young. World Scientific (Singapore, 1997).
  - [19] F. Cooper, B. Freedman and D. Preston, Nucl. Phys. **B210**, 210 (1989).

---

Authors	$J$ -Distribution/Material	$\nu$	$\eta$
This Work ((10, 20) pair)	$\pm J$	2.15(15)	-0.337(15)
Gunnarsson et al. [5]	$\text{Fe}_{0.5}\text{Mn}_{0.5}\text{TiO}_3$	1.69(15)	-0.36(7)
Palassini-Caracciolo [12]	$\pm J$	1.8(2)	-0.26(4)
Marinari-Parisi-Ruiz-Lorenzo [9]	Gaussian	2.00(15)	-0.36(6)
Berg-Janke [11]	$\pm J$	—	-0.37(4)
Kawashima-Young [7]	$\pm J$	1.7(3)	-0.35(5)
Iñiguez-Parisi-Ruiz-Lorenzo [8]	Gaussian	1.5(3)	—
Ogielski [13]	$\pm J$	1.3(1)	-0.22(5)
Bhatt-Young [14]	$\pm J$	1.3(3)	-0.3(2)
Bhatt-Young [15]	Gaussian	1.6(4)	-0.4(2)

---

TABLE III. Critical exponents from experiments and numerical simulations.

- [20] See for instance M.N. Barber in *Phase Transitions and Critical Phenomena*, vol. 8, edited by C. Domb and J.L. Lebowitz (Academic Press, London, 1983).
- [21] M. Lüscher, P. Weisz and U. Wolff, Nucl. Phys. **B359** 221 (1991); J.-K. Kim, Phys. Rev. Lett. **70**, 1735 (1993); S. Caracciolo, R. G. Edwards, S. J. Ferreira and A. Sokal, Phys. Rev. Lett. **74**, 2969 (1995); S. Caracciolo, R. G. Edwards, and A. Sokal, Phys. Rev. Lett. **75**, 1891 (1995).
- [22] H. G. Ballesteros, L. A. Fernández, V. Martín-Mayor and A. Muñoz Sudupe, Phys. Lett. **B378**, 207 (1996); Nucl. Phys. **B483**, 707 (1997).
- [23] J. Kisker, L. Santen, M. Schreckenberg and H. Rieger, Phys. Rev. B **53**, 6418 (1996); E. Marinari, G. Parisi, J. J. Ruiz-Lorenzo and F. Ritort, Phys. Rev. Lett. **76**, 843 (1996); Y. G. Joh, R. Orbach, G. G. Wood, J. Hammann and E. Vincent, Phys. Rev. Lett. **82**, 438 (1999); G. Parisi, E. Marinari, F. Ricci-Tersenghi and J. J. Ruiz-Lorenzo J. Phys. A. **33**, 2373 (2000).
- [24] H. G. Ballesteros, L. A. Fernández, V. Martín-Mayor, A. Muñoz Sudupe, G. Parisi and J. J. Ruiz-Lorenzo, Phys. Lett. **B400**, 346 (1997); Nucl. Phys. **B512[FS]**, 681 (1998) ; Phys. Rev. **B58**, 2740 (1998).
- [25] E. Marinari, V. Martín-Mayor and A. Pagnani, cond-mat/0002327, to be published in Phys. Rev. **B**.
- [26] F. Ritort and M. Sales, cond-mat/0003336.
- [27] K. Binder, Z. Phys. B **43**, 119 (1981).
- [28] E. Marinari, C. Naitza, G. Parisi, M. Picco, F. Ritort and F. Zuliani, Phys. Rev. Lett. **81**, 1698 (1998).
- [29] J. Pech, A. Tarancón and C. L. Ullod, Comput. Phys. Commun. **106**, 10 (1997).
- [30] J. J. Ruiz-Lorenzo and C. L. Ullod. Comput. Phys. Commun. **125**, 210 (2000).
- [31] A. Cruz, J. Pech, A. Tarancón, P. Téllez, C. L. Ullod, C. Ungil, cond-mat/0004080, submitted to Comput. Phys. Commun.
- [32] H. G. Ballesteros and V. Martín-Mayor, Phys. Rev. E **58**, 6787 (1998).
- [33] One of the Schwinger-Dyson equations for a spin glass reads as:

$$\frac{1}{V} \overline{\left\langle \sum_i e^{-2\beta\sigma_i S_i} \right\rangle} = 1, \quad S_i \equiv \sum_{j \text{ n.n. } i} J_{ij} \sigma_j,$$

where the sum ( $\sum_{j \text{ n.n. } i}$ ) is performed over all the six nearest neighbors of the site  $i$ .

- [34] If we denote the coordinates of a given spin  $(x, y, z)$  by  $i \equiv x + yL + zL^2$ , the coordinates of the three nearest neighbors (in the three positive directions) are given by:  $i_1 = (i + 1) \bmod L^3$ ,  $i_2 = (i + L) \bmod L^3$  and  $i_3 = (i + L^2) \bmod L^3$ .
- [35] M. Falcioni, E. Marinari, M. L. Paciello, G. Parisi and B. Taglienti, Phys. Lett. **B108**, 331 (1982); A. M. Ferrenberg and R. H. Swendsen, Phys. Rev. Lett. **61**, 2635 (1988).
- [36] A. D. Sokal, *Bosonic Algorithms in Quantum Fields on the Computer*. Advanced Series on Directions in High Energy Physics, Vol 11, edited by M. Creutz. (World Scientific, Singapore 1992).
- [37] We have simulated the two dimensional XY model using the Wolff single cluster algorithm [38]. We have done different runs, near the critical point  $\beta \simeq 1.11$ , on lattice sizes  $L = 16, 32$  and  $64$ , using the spectral density method in the analysis of the data.
- [38] U. Wolff, Phys. Rev. Lett. **62**, 361 (1989).
- [39] The leading correction to scaling is given by the universal exponent  $\omega$ . However, the nonlinear dependence of the scaling fields over the couplings of the Hamiltonian and the analytic part of the free energy provided two sources of additional scaling corrections. Considering for instance the susceptibility, one has that the leading exponents for the analytic scaling-corrections (from each one of the above mentioned sources) are respectively:  $\gamma/\nu + d - 1/\nu$  and  $\gamma/\nu$ . In our model they are approximately 4.7 and 2.3 (resp.). These figures are much bigger than our estimate for the  $\omega$  exponent, which is 0.84(43), so that we check, a posteriori, that they could be safely neglected. We address to Ref. [40] for a detailed study on the analytic scaling-corrections.
- [40] J. Salas and A. D. Sokal, cond-mat/9904038 version 1.